Veterinary Immunology and Immunopathology 222 (2020) 110035

Contents lists available at ScienceDirect

Veterinary Immunology and Immunopathology

journal homepage: www.elsevier.com/locate/vetimm

Immunopathological characterization of red focal changes in Atlantic salmon (*Salmo salar*) white muscle

Håvard Bjørgen[a], Subramani Kumar[b], Gjermund Gunnes[a], Charles McL. Press[a], Espen Rimstad[c], Erling Olaf Koppang[a,*]

[a] Department of Basic Science and Aquatic Medicine, Faculty of Veterinary Medicine, Norwegian University of Life Sciences, Oslo, Norway
[b] Centre for Biotechnology, Anna University, Chennai, 600 025, India
[c] Department of Food Safety and Infection Biology, Faculty of Veterinary Medicine, Norwegian University of Life Sciences, Oslo, Norway

ARTICLE INFO

Keywords:
Atlantic salmon
Inflammation
Piscine orthoreovirus

ABSTRACT

Farmed Atlantic salmon (*Salmo salar*) are prone to various conditions affecting the quality of the fillet. A well-known but so far poorly understood condition is the focal red changes in muscle, often referred to as *haemorrhages*. Such changes are characterized by muscle necrosis, haemorrhages and acute inflammation. They can progress into *focal melanised changes*, a chronic inflammatory condition with melanin-producing leukocytes. The initial cause of intramuscular haemorrhages is unknown. In this study, we aimed to reveal some of their key immunological features. Samples of red focal changes were investigated by immunohistochemistry (IHC), *in situ* hybridization (ISH) and RT-qPCR for various immune markers. The results were compared with samples of melanised changes and control muscle, subjected to the same analyses. In all red changes, infiltrates with mononuclear cells were detected, consisting mostly of MHC class I/II$^+$ cells, but also of CD3$^+$ and CD8$^+$ cells. ISH studies on IgM showed few to moderate amounts of B-cells in red focal changes. Trends in the RT-qPCR showed upregulation of genes related to innate immunity in the red changes, whereas genes related to adaptive immunity were upregulated in the melanised changes. An important result was the significant downregulation of the anti-inflammatory cytokine IL10 in all red changes. Our findings indicate that we can rule out an auto invasive nature of the changes. The downregulation of IL10 at an early phase is a trait for the condition.

1. Introduction

Abundant melanin production may occur with chronic inflammatory conditions in ectothermic species. Chronic inflammation in the muscle of salmon (*Salmo salar*) may result in melanised focal changes in the fillet, which are commonly termed *black spots* (Larsen et al., 2012). With an occurrence of approximately 20 % of the fillets at slaughter, such changes are regarded as the most costly quality problem by the salmon industry (Mørkøre et al., 2015).

The hallmark of the inflammatory changes associated with melanised focal changes in skeletal muscle is the presence of melano-macrophages, which are melanin-containing macrophage-like cells found in ectothermic vertebrates (Bjørgen et al., 2019; Larsen et al., 2012). Most melanised focal changes occur in the cranio-abdominal region of the fillet and seem to develop from acute intramuscular haemorrhages, *i.e.* red focal changes, which over time progress into chronic melanised foci (Bjørgen et al., 2019, 2015). Red focal changes occur less frequent than melanised changes and have a prevalence of about 4 % throughout the production period in seawater (Bjørgen et al., 2019).

An earlier study of both red- and melanised focal changes collected at time of slaughter showed a range of macroscopic appearance from red to black discolouration, where all foci contained varying degrees of inflammatory cells, haemorrhage, myocyte regeneration, fibrosis and melanisation (Bjørgen et al., 2015). These findings linked the two conditions and strengthened the hypothesis of a transition from an acute red to a chronic melanised inflammatory manifestation. *Piscine orthoreovirus* (PRV) antigen was detected by immunohistochemistry (IHC) in all foci, whilst no other viruses were found, leaving PRV as the sole common viral denominator. PRV was detected in both acute haemorrhagic changes and in chronically inflamed changes with fibrosis and melanisation and was even found encapsulated within well-organised granulomas (Bjørgen et al., 2015). The virus was observed as

* Corresponding author at: Section of Anatomy and Pathology, Institute of Basic Sciences and Aquatic Medicine, Faculty of Veterinary Medicine, Norwegian University of Life Sciences, Ullevålsveien 72, Oslo, Norway.
E-mail addresses: havard.bjorgen@nmbu.no (H. Bjørgen), kumar.subramani@mcgill.ca (S. Kumar), gjermund.gunnes@nmbu.no (G. Gunnes), charles.press@nmbu.no (C.M. Press), espen.rimstad@nmbu.no (E. Rimstad), erling.o.koppang@nmbu.no (E.O. Koppang).

https://doi.org/10.1016/j.vetimm.2020.110035
Received 16 September 2019; Received in revised form 26 February 2020; Accepted 6 March 2020

Table 1
Primary antibodies used for immunohistochemical analysis.

	Antibody/dilution	Reactive against	Reference
PRV	Anti-PRV - σ1, 1:600	Capsid protein σ1	(Finstad et al., 2012)
	Anti-PRV - μNS, 1:2200	Non-structural protein μNS	(Haatveit et al., 2016)
Immune molecules	Sasa MHC class I F3-31, 1:20	Alpha 3 domain of MHC I alpha chain	(Hetland et al., 2010)
	Sasa MHC class II F1-12, 1:400	Beta 2 domain of MHC II beta chain	(Hetland et al., 2010)
	Anti-CD3, 1:400	Epsilon chain of the CD3 transmembrane protein	(Boardman et al., 2012)
	Sasa CD8 F1-29, 1:100	CD8α, a part of the CD8 complex	(Hetland et al., 2010)

globular cytoplasmic inclusions within macrophage-like cells and erythrocytes. These inclusions resemble viral factories which is the site of viral replication (Haatveit et al., 2016). A recent study on the development of discoloured muscle changes during the seawater phase has confirmed the presence of PRV in granulomatous melanised changes, but also showed that red- and low-grade melanised focal changes could occur without the presence of PRV, indicating that viral infection is not the initial cause of the myositis (Bjørgen et al., 2019). As studies on red focal changes are limited, it seems crucial to obtain more knowledge on these early-stage haemorrhages.

Red focal changes have been shown to occur in different macroscopic grades, ranging from small intramuscular haemorrhages to larger haematomas (Bjørgen et al., 2019, 2015). Histologically, all changes are characterised by similar pathological changes including acute necrosis of myocytes, extravascular erythrocytes, activated fibroblasts and endomysial and perimysial infiltration of leukocytes (Bjørgen et al., 2019). Based on their morphology, most leukocytes are thought to be macrophage-like cells undergoing myophagocytosis, but the presence of other leukocyte populations has so far not been studied.

With an unknown aetiology, this study aimed to reveal the immunopathological features of red focal changes. In humans, a number of different immune-related diseases are common in the musculoskeletal system (Dalakas, 2015), but such conditions have not been explored in fish. Here, we identify key innate, adaptive and anti-viral immune responses by applying immunohistochemistry (IHC), *in situ* hybridization (ISH) and RT-qPCR for different immune markers and genes. PRV is ubiquitous in farmed Atlantic salmon in Norway in the marine phase and the study was performed on PRV-positive fish. A group of fish with melanised focal changes (also PRV-positive) was included in the investigations, allowing a comparison between the acute and the chronic manifestation of the condition. As bacteria have previously been suggested to contribute to the pathogenesis of the condition (Krasnov et al., 2016), ISH was used to investigate for the presence of bacteria in red focal changes. Our study reveals important immunological features in red focal changes and provides novel information on the initial phase of this very costly condition.

2. Materials and methods

2.1. Fish groups and samples

Muscle samples from three different fish groups from our previous investigation were used in the current study (Groups A, C and H from (Bjørgen et al., 2015)). Group A consisted of samples of primarily melanised focal changes, while Group C consisted of samples of red focal changes. Both groups originated from fish that were positive for PRV-1 by RT-qPCR (Bjørgen et al., 2015). The groups came from different farm sites on the coast of Norway and were collected at fish abattoirs. A population of PRV-negative wild salmon without any detectable pathological changes (Group H) was acquired from the Drammen River in Eastern Norway. Details for the different groups have been published earlier (Bjørgen et al., 2015).

The groups were originally large, but for the purpose of in-depth immunological investigations, an arbitrary sub-selection from each group was made consisting of six red muscle changes from Group C (n = 6) and six melanised muscle changes from Group A (n = 6). These samples were used for both histological and gene expression studies. White muscle tissue from one fish in Group H (n = 1) served as negative control material for IHC/ISH experiments, as this sample was both PRV-negative and free from any observable pathological changes. For RT-qPCR experiments, muscle samples (6 from Group A and 6 from Group C with no visible changes) obtained from same anatomical location in the contralateral fillet were used as control material.

2.2. Histology and immunohistochemistry (IHC)

All samples were collected on 10 % phosphate-buffered formalin, routinely processed and paraffin-embedded after 24 h. Sections were cut 2 μm thick and mounted on glass slides, incubated for 24 h at 37 °C, de-waxed in xylene and rehydrated in graded alcohol baths and stained according to standard procedures with haematoxylin and eosin-staining (HE). The histological characteristics of the changes and controls have previously been described (Bjørgen et al., 2015).

Sections were cut 4 μm thick and mounted on glass slides (Superfrost + ©, Mentzel, Braunshweig, Germany), incubated for 24 h at 37 °C and thereafter for 30 min at 58 °C, de-waxed in xylene and rehydrated in graded alcohol baths before being transferred to distilled water. Sections were autoclaved in 0.01 M citrate buffer, pH 6.0 at 120 °C for 10 min, followed by treatment with phenylhydrazine (0.05 %; Sigma-Aldrich, St. Louis, MO, USA) for 40 min at 37 °C. The slides were rinsed three times in phosphate-buffered saline (PBS).

Nonspecific binding was prevented by blocking with goat normal serum diluted 1:50 in 5 % bovine serum albumin (BSA) in PBS. A primary antibody (Table 1) was diluted in tris-buffered saline (TBS) with 1 % BSA and added to the slides and incubated for 30 min. The sections were rinsed three times in TBS and incubated with a secondary antibody (EnVision© System kit; Dako, Glosrup, Denmark) for 30 min. The slides were washed three times in TBS and incubated with DAB or AEC for 7 or 14 min, respectively (EnVision© System kit), to evoke colour reaction (brown or red). Sections were washed with distilled water and counterstained with Mayer's haematoxylin for 1.5 min and mounted with Aquatex® (Merck KGaA, Darmstadt, Germany).

Negative control sections were incubated with 1% BSA or rabbit serum collected prior to immunization, instead of the primary antibody. For the PRV-staining, heart tissue collected from an heart and skeletal muscle inflammation (HSMI, where PRV is causative (Wessel et al., 2017)) challenge trial was used as positive control (Finstad et al., 2014).

2.3. Scoring of IHC

The muscle samples were scored using a semi-quantitative system. Each section was given a value between 0–3 according to the presence of immune-labelled cells. Value 0 was given when there was no observable labelling. When a low number of immune-labelled cells were present, the sample was scored with value 1. When labelling was moderate, with scattered single labelled cells in addition to focal or multifocal infiltrates, the sample was scored with value 2. When labelled cells were abundant in the section, with large numbers of single labelled cells in addition to multifocal infiltrates, the sampled was

scored with value 3.

2.4. ISH of IgM and 16S rRNA

Sections were cut 4 μm thick and mounted on glass slides (Superfrost + ©). To detect IgM RNAs, the slides underwent hybridization with a probe based on Atlantic salmon IgM sequence (Ssa-LOC106606767 targeting 219–1157 of XM_014203125) designed by ACDBio RNAscope® (Newark, CA). The sequence was chosen to detect RNA for both secreted and membrane-bound forms and all sub-variants of IgM. The probe targeting 16S rRNA was ordered from RNAscope® Catalog Probe List catalog number #464,461, confirmed as a universal target for bacteria. The method was performed using RNAscope RED 2.5 according to the manufacturer's instructions (Wang et al., 2012). Mid kidney was included as positive control tissue for the IgM probe. Head-kidney from fish with a systemic bacterial diagnosis (provided by the Norwegian Veterinary Institute) was used as control material for the 16S rRNA probe. RNAscope® Negative Control probe catalog number #701,021 was included to confirm absence of background and/or non-specific cross-reactivity in the samples.

2.5. RT-qPCR

Red and melanised focal changes (affected) and corresponding (unaffected) control muscle were collected and immersed into RNAlater solution. The samples were stored at −20 °C until RNA extraction.

The total RNA was extracted using QIAzol® Lysis Reagent. According to the manufacturer's recommendation, the extracted total RNA was dissolved in nuclease-free water. The total RNA was estimated using Nanodrop Spectrophotometer at the wavelength of 260 and 280 nm. Only RNA with an absorbance ratio A260:A280 greater than 1.9 were used for the reverse transcription. The total RNA was converted into cDNA as per the manufacturer's recommendations for QuantiTect® Reverse Transcription. Total RNA (750 ng) was aliquoted into 0.2 ml sterile PCR reaction tubes and DNA wipeout (2 μl) buffer was added. The total reaction volume was made up to 14 μl with nuclease free water. The cDNA reaction tube was incubated at 42 °C for 8 min in Thermal cycler and then immediately placed on ice for 10 min. The first-strand cDNA synthesis reverse-transcription cocktails (Quantiscript Reverse Transcriptase 1 μl Quantiscript RT buffer 5 × 4 μl and RT primer mix 1 μl) were aliquoted 6 μl into each reaction tube. The conditions used were 37 °C for 30 min and 95 °C for 3 min. After successive completion of reverse-transcription reactions, the cDNA cocktail was stored on ice before performing qPCR analysis and reverse-transcription reactions cocktail stored at −20 °C for long-term storage. The cDNA was used as a template for further amplification using RT-qPCR with specific primers targeting key innate, adaptive and anti-viral immune genes (Table 2).

Evaluation of gene expression was carried out using specific gene primers in Agilent Mx3005P-Stratagene qPCR instruments. cDNA of each experimental group was used in triplicate along with EF1AB as an internal control. A negative control reaction was performed for all the primers excluding of the cDNA template. The amplifications were carried out in a 96 well plate with a total volume of 13 μl in each well, using cDNA, 2 pmol of each gene-specific primer pair with TaqMan™ Universal PCR Master Mix (Thermo Fisher Scientific) and DEPC water. The following thermal cycling conditions were used: 95 °C for 10 min, 95 °C for 15 s, 58 °C for 15 s and 60 °C for 60 s for 40 cycles. After amplification, relative expression levels of CD4-2a, CD8, MHC class I, MHC class II, Viperin, Mx1, IFNγ, TNFα, IL1b, IL10 and Casp3 were estimated. The relative fold of induction was determined by ΔΔCT method, allowing a quantification of the expression of the genes of interest against the reference gene (EF1AB) by means of fold change. The fold (mean ± SD, n = 6) change was calculated using the formula 2- ΔΔCT. The testing method used was One-way ANOVA. Statistical significance was calculated by the Dunnett's multiple comparisons test.

3. Results

3.1. Immunohistochemistry – red focal changes

Two different PRV proteins were targeted by IHC: the structural protein σ1 and the non-structural protein μNS. The latter is not a part of viral particles and thus indicates active viral replication. In red changes, the σ1 labelling scored between 2–3, *i.e.* moderate to high amounts of immune-labelled cells (Table 3), while μNS labelling revealed a similar pattern (Fig. 1A). The μNS$^+$ cells displayed a distinct, cytoplasmic and globular label (Fig. 1B).

Moderate to high amounts (scored 2–3) of MHC class I and II$^+$ cells were detected in all changes (Table 2). MHC class I$^+$ cells were widely distributed in and around necrotic myocytes in the connective tissue (Fig. 2A), phenotypically resembling macrophage-like cells, with a single oval nucleus located eccentrically. Focal accumulations of MHC class I$^+$ were frequent (Fig. 2B). All myocytes and erythrocytes were MHC class I$^-$, but the endothelial lining of intra-muscular capillaries were MHC class I$^+$, consistent with results from previous studies (Hetland et al., 2011, 2010). Scattered MHC class II$^+$ cells were found throughout the changes both in the myomeres and in the connective tissue of the myosepta (Fig. 2C). MHC II$^+$ cells were also encountered in focal accumulations (Fig. 2D) where MHC class I reactivity was seen in the same foci.

Immunolabelling for T cells varied significantly within the red focal changes, though immunolabelled cells were detected in all individuals (Table 3). Large amounts of CD3$^+$ cells (scored 3) were detected in three out of six samples. CD8$^+$ cells occurred in different amounts in four of the samples. Only one of the changes had large amounts of CD8$^+$ cells (scored 3). Serial sections of a highly reactive red focal change showed severe myocyte necrosis and multifocal inflammation (Fig. 3A). The infiltrate contained numerous cells labelled for PRV (Fig. 3B) and displayed strong labelling for MHC class II (Fig. 3C). T cells appeared abundantly in the same infiltrate (Fig. 3D) and many cells were CD8$^+$ (Fig. 3E). The unaffected virus negative control muscle was negative for all antibodies, except MHC class I, where occasional immunolabelled cells were present in the perimysium (data not shown).

3.2. Immunohistochemistry – melanised focal changes

Immunolabelling for PRV with two different antibodies (anti-σ1 and anti-μNS) displayed immunolabelled cells in all melanised focal changes (data not shown). The score varied (from 1 to 3) with the stage of the inflammation: severe muscle changes with degeneration, necrosis and multiple leukocyte infiltrates generally received a high score, while in highly fibrotic changes with less degeneration and fewer leukocytes had only scattered immunolabelled cells and a lower score. Nodular granulomas were found in several changes (Fig. 4A). μNS$^+$ cells were detected among inflammatory cell infiltrates but were also present centrally in the granulomas (Fig. 4B), indicating replication of virus within such changes. Further, the granulomas displayed phenotypic features typical of an active immunological site, with strong immunolabelling for MHC class I (Fig. 4C), a central core of MHC class II$^+$ cells (Fig. 4D) with surrounding CD3$^+$ cells (Fig. 4E) and occasional CD8$^+$ cells (Fig. 4F).

3.3. In situ hybridization – IgM in red and melanised focal changes

IgM$^+$ cells were found in all changes in varying amounts. Most of the labelled cells had a characteristic lymphocyte-like phenotype with a prominent round nucleus and scant cytoplasm. In the red changes, few to moderate numbers of labelled cells were seen in most changes except one which contained many IgM$^+$ cells (Fig. 5A). In all melanised changes, many IgM$^+$ cells were detected within the granulomatous inflammation (Fig. 5B). Mid kidney control tissue contained numerous IgM$^+$ cells. Negative controls showed no labelling of cells.

Table 2
Sequences of primers and probes used in quantitative real-time RT-PCR analysis.

Gene	Sequence (5´- 3´)	Reference
$EF1A_B$	F-TGCCCCTCCAGGATGTCTAC R-CACGGCCCACAGGTACTG P-FAM-AAATCGGCGGTATTGG-MGB	(Olsvik et al., 2005)
CD4-2a	F-GCCCCTGAAGTCCAACGAC R-AGGCTTCTCTCACTGCGTCC P-FAM-CCGCACACTAGAGGGTCCACCACG-BHQ	(Aas et al., 2014)
CD8a	F-ACTTGCTGGGCCAGCC R-CACGACTTGGCAGTTGTAGA P-CGACAACAACAACCACCACG-BHQ	(Aas et al., 2014)
MHC-I	F-GGAAGAGCACTCTGATGAGGACAG R-CACCATGACTCCACTGGGGTAG P-TCAGTGTCTCTGCTCCAGAAGACCCCCT-BHQ	(Aas et al., 2014)
MHC-II	F-CCACCTGGAGTACACACCCAG R-TTCCTCTCAGCCTCAGGCAG P-FAM-TCCTGCATGGTGGAGCACATCAGC-BHQ	(Aas et al., 2014)
IL-1b	F-GCTACCACAAAGTGCATTTG R-GAGGTTGGATCCCTTTATGC P-FAM-CCATTGAGACTAAAGCCAGACCTGTAG-BHQ	(Moldal et al., 2014)
IL-10	F-GAAACATCTTCCACGAGCTG R-GTCCAGCTCTCCCATTGC P-FAM-TTCTCCTGTAAGAAACCGTTTGACATC-BHQ	(Aas et al., 2017)
Mx1	F-GATGCTGCACCTCAAGTCCTATTA Rev-CACCAGGTAGCGGATCACCAT P-FAM-GCTGATCAGATTCCCATGGT-BHQ	(Wessel et al., 2017)
Viperin	F-AGCAATGGCAGCATGATCAG R-TGGTTGGTGTCCTCGTCAAAG FAMAGTGGTTCCAAACGTATGGCGAATACCTGBHQ	(Austbø et al., 2014)
TNFa	F-GCAGCTTTATGTGCGGCAG R-TTTTGCACCAATGAGTATCTCCAG P-FAM-TGGAAGACTGGCAACGATGCAGGA-BHQ	(Moldal et al., 2014)
IFNg	F AGGACACACCTGCAGAACCTG R AGTTTGGAGGCTTTCTCGTAGATG FAM-AGTCCAGGGGAAGGCTCTGTCCG-BHQ	(Austbø et al., 2014)
Casp3[†]	F-AGTGAAGGTTGCCAATGACC R-ACATTGCCATCTGTGCCATA	NM_001139921.1

[†] SYBR green primers that were analysed using corresponding SYBR green EF1AB housing keeping primers.

Table 3
Scoring of IHC from muscle samples. Values 0-3 indicate respectively no labelled cells (0); few labelled cells (1); moderate amounts of labelled cells (2); and large amounts of labelled cells (3).

	Fish	PRV σ1	PRV μNS	CD3	CD8	MHC class I	MHC class II
	Control	0	0	0	0	1	0
Red focal changes	I	2	3	3	2	3	2
	II	3	3	3	1	1	3
	III	2	2	2	0	2	2
	IV	2	1	1	0	2	3
	V	3	3	3	3	3	3
	VI	3	2	1	1	2	2
Melanised focal changes	I	3	3	3	2	2	3
	II	1	1	3	1	2	2
	III	2	1	1	1	2	2
	IV	3	2	2	1	2	3
	V	3	3	2	1	2	2
	VI	2	2	2	1	2	3

3.4. Investigations on bacterial presence - in situ hybridization targeting 16S rRNA and Gram stain

Scattered bacteria-like structures were occasionally detected within intact myocytes and in cells in the endomysium in some red (Fig. 6A) and melanised changes. These bacteria-like structures were not commonly found in relation to pathological changes but appeared randomly distributed throughout the tissue in both red and melanised changes. Most changes did not show labelling for 16S rRNA (Fig. 6B). Gram stain in parallel sections did not reveal the presence of bacteria. Positive controls demonstrated labelling for bacteria (Fig. 6C).

3.5. RT- qPCR analysis of red and melanised focal changes

Gene expression of selected immune- and anti-viral genes were investigated in both red and melanised changes and in unaffected control muscle. The individual variation was high for most genes, but with some trends for different groups (Fig. 7). For genes related to acute, innate immune responses, IL1b and TNFα expression were upregulated in some individuals in both red and melanised changes and were highest in the red changes. There was a highly significant down-regulation of IL10 in the red changes ($P < 0.0001$), while a modest increase of IL10 was present in the melanised changes ($P < 0.05$).

For genes related to adaptive immunity, a statistically significant increase in CD4 was detected in both red and melanised changes when compared to unaffected muscle. CD8, MHC class I and II were generally upregulated in the melanised changes (statistically significant for MHC class II, $P < 0.05$) and a similar trend was not found in the red changes.

For innate antiviral genes, Mx1 and Viperin expression varied a lot between individuals and no clear trends were detected in either group. INFγ was downregulated in all melanised changes ($P > 0.05$), while the red changes showed a diverse INFγ expression. An increase in gene expression of Casp3 was seen in all red changes, though not statistically significant.

4. Discussion

The immune response in melanised focal changes in Atlantic salmon has been investigated previously in both histologic and transcriptomic studies (Krasnov et al., 2016; Larsen et al., 2012). However, this is the first report on the immune characterization of red focal changes. In comparison with melanised focal changes, the immunological features

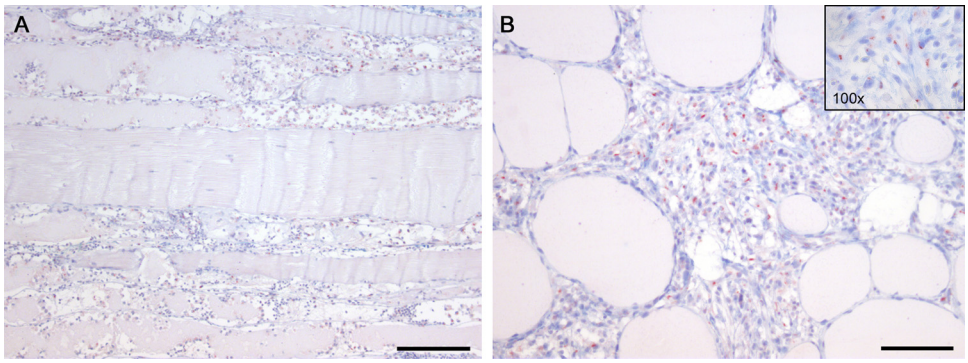

Fig. 1. PRV μNS immunolabelling of a red focal change. A) Abundant amounts of PRV$^+$ cells (red) in the necrotic muscle tissue, in addition haemorrhage and degenerated myocytes. Scale bar = 100 μm. B) PRV$^+$ cells (red) are present in a dense infiltrate of leukocytes. High magnification image shows distinct and globular immunolabelling in the cytoplasm of mostly macrophage-like cells. Scale bar = 50 μm (For interpretation of the references to colour in this figure legend, the reader is referred to the web version of this article.).

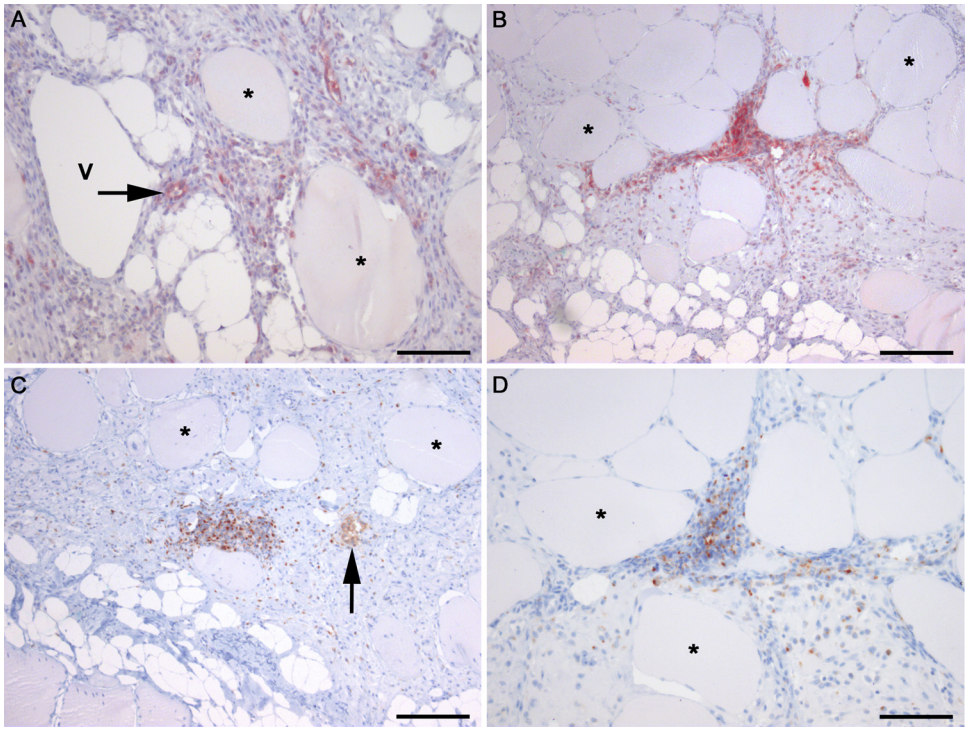

Fig. 2. MHC class I (A and B) and II (C and D) immunolabelling in red focal changes. A) Abundant amounts of MHC class I$^+$ cells (red) are present in the inflamed muscle tissue. The cells are distributed in a scattered manner, as well as in focal clusters. Immunolabelling is also seen in the endothelial lining of intramuscular vessels (arrow). V = vacuole. Scale bar = 50 μm. B) A dense, focal cellular infiltrate (red) is present in the necrotic muscle tissue. Degenerated myocytes with MHC class I$^+$ cells (red) are evident near the fatty tissue of the myosepta. Scale bar = 100 μm. C) Scattered and focal accumulations of MHC class II$^+$ cells (brown) appear abundantly in the necrotic muscle tissue. Immunolabelled cells in a degenerated myocyte are indicated (arrow). Scale bar = 100 μm. D) A focal infiltrate of MHC class II$^+$ cells. Scale bar =50 μm. Examples of myocytes are indicated by asterisks (For interpretation of the references to colour in this figure legend, the reader is referred to the web version of this article.).

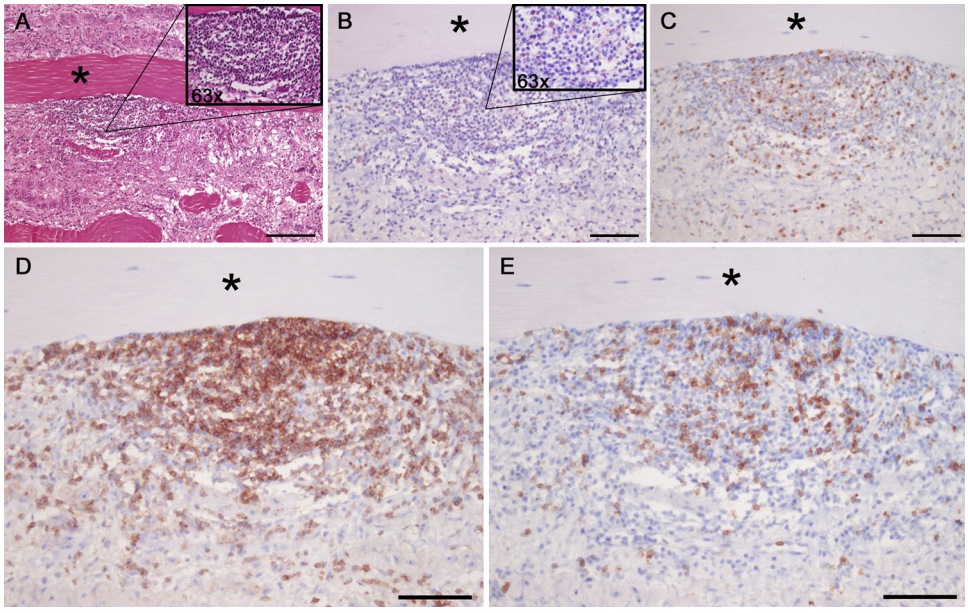

Fig. 3. Serial transverse sections of a red focal change. A large, central infiltrate of leukocytes is present and the change scored 3 on PRV-, MHC class I and II-, CD3- and CD8 IHC labelling. Asterisk in A-E marks a myocyte. A) A degenerated and necrotic musculature with a dense focus of leukocytes beneath an intact myocyte (asterisk). Higher magnification (63 x) image in the upper right corner. H&E stain. Bar = 100 μm. B) Multiple PRV$^+$ macrophage-like cells (red) in an area with abundant leukocytes. PRV σ1 immunolabelling. Bar = 50 μm. C) Multiple MHC class II$^+$ cells (brown) in an area with abundant leukocytes. MHC class II immunolabelling. Bar = 50 μm. D) Large amounts of CD3$^+$ cells (brown) within an infiltrate of leukocytes. CD3 immunolabelling. Bar = 50 μm. E) Multiple CD8$^+$ cells (brown) in an infiltrate of leukocytes. CD8 immunolabelling. Bar = 50 μm (For interpretation of the references to colour in this figure legend, the reader is referred to the web version of this article.).

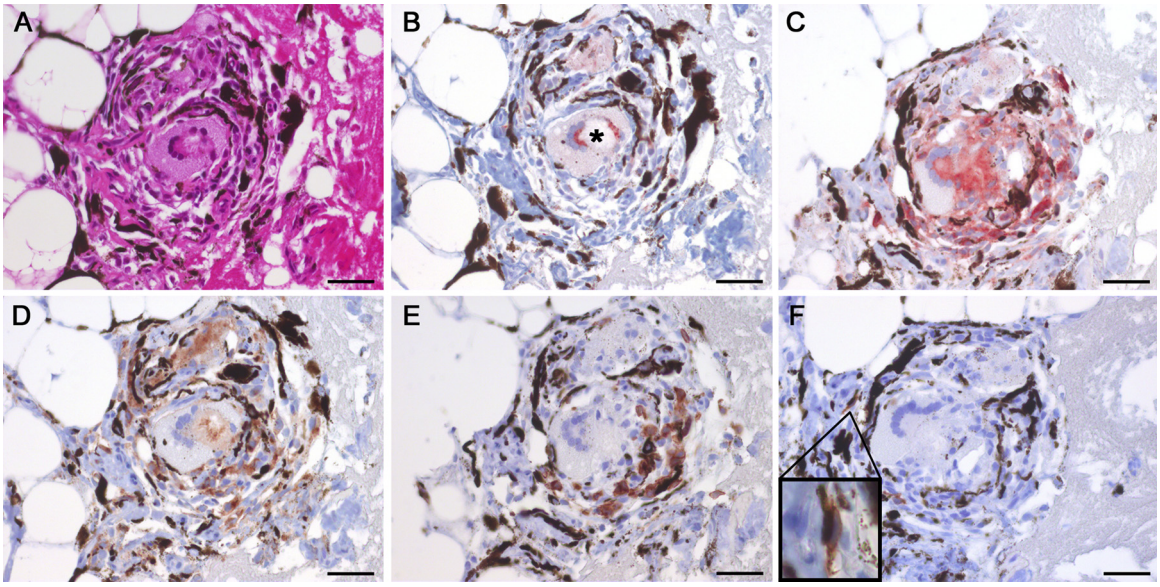

Fig. 4. Immunolabelling of a nodular granuloma in a melanised focal change. A) A round to oval granuloma located in the periphery of a myotome towards the myoseptum. The cell-rich granuloma is heavily melanised and contains a central core with necrotic debris and a multi-nucleated giant-cell. H&E staining. B) PRV$^+$ cells (red) are present in the granuloma centre (asterisk). Immunolabelled cells are evident in relation to a multi-nucleated giant cell. PRV μNS immunolabelling. C) Abundant MHC class I$^+$ cells (red) in both peripheral and central parts of the granuloma. MHC class I immunolabelling. D) Numerous MHC class II$^+$ cells are present within the granuloma (brown). MHC class II immunolabelling. E) Immunolabelled T lymphocytes surround the central core the granuloma and are associated with the fibrous capsule of the granuloma. CD3 immunolabelling. F) A few CD8+ cells are present in the in the outer fibrous capsule of the granuloma. High magnification picture of an immunolabelled cell is shown in the lower left corner. CD8 immunolabelling. Scale bar (A-F) = 20 μm (For interpretation of the references to colour in this figure legend, the reader is referred to the web version of this article.).

of red focal changes suggested a tissue site in transition from an acute to chronic inflammation. IHC showed a varied presence of immune cells in red changes while melanised changes were dominated by granulomatous inflammation, including highly organized granulomas. The non-structural PRV protein μNS was detected in structures resembling viral factories, which are specialized structures where PRV replicates and new viral particles are assembled. The viral factory-like structures were found in both red and melanised changes. Furthermore, immune genes associated with innate, adaptive and innate anti-viral immunity showed that expression of the anti-inflammatory cytokine IL10 was down regulated (statistically significant $P < 0.0001$) in all red changes and upregulated in all melanised changes.

The samples in our study were collected at slaughter and thus PRV-positive, and representative for farmed Atlantic salmon in Norway, where PRV is ubiquitous (Løvoll et al., 2012). The non-structural protein μNS was targeted by IHC to address the presence of replicating PRV. The protein was found in both red and melanised changes in various amounts indicating an on-going replication even in the highly organized granulomas. Positive signal occurred as cytoplasmic inclusions, *i.e.* resembling viral factories (Haatveit et al., 2016). The presence of PRV specific RNA has been shown previously by ISH in granulomatous melanised changes (Bjørgen et al., 2019); here we indicate that PRV replication occurs in red changes. Importantly, we know that red changes can develop without PRV infection and therefore, we cannot attribute the presence of replicating virus as the cause for the condition and that there may be several causes for development of red changes (Bjørgen et al., 2019). On the other hand, the development of chronic melanised changes has been associated with local persistence and replication of PRV (Bjørgen et al., 2019), thus possibly acting as the constant trigger of inflammation.

The presence of immune cells was investigated in both red and melanised changes. Various amounts of MHC class I and II and T cells were detected in all changes and they often occurred in highly reactive foci. This was reflected by the PCR results, where substantial individual variation was observed, however, the lack of homogeneity in these changes is an intrinsic unknown factor for the interpretation of the RT-qPCR results. Diversity within the changes could easily be visualised by histology, however, such information is lost in tissue extractions and PCR analysis. The appearance of focal accumulations of immune cells, as seen in the immunolabelling, could have a large effect on the RT-qPCR results pending upon the sampling. Therefore, histological investigations are necessary when studying heterogenic tissue like

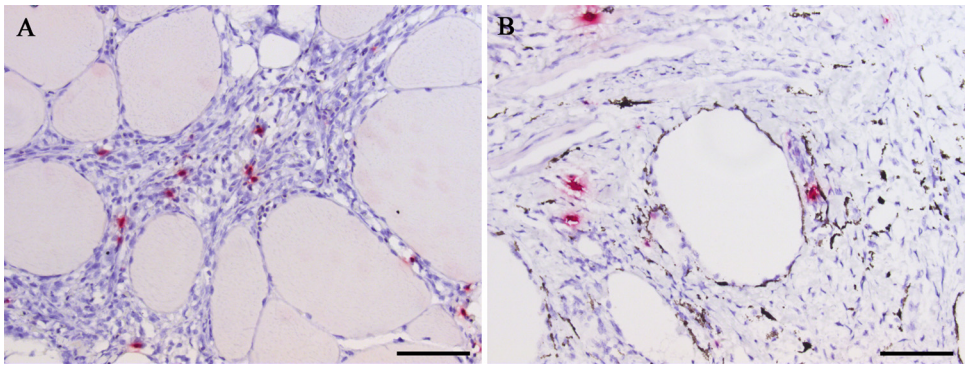

Fig. 5. *In situ* hybridization – IgM in red and melanised focal changes. A) IgM$^+$ cells in a highly reactive inflammatory focus in a red focal change. Bar =50 μm. B) IgM$^+$ cells scattered around a vacuole surrounded by numerous melano-macrophages. Bar = 50 μm (For interpretation of the references to colour in this figure legend, the reader is referred to the web version of this article.).

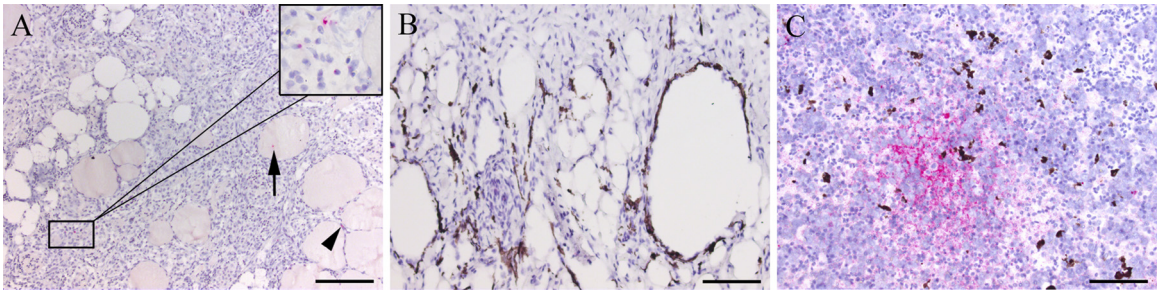

Fig. 6. *In situ* hybridization - 16 s rRNA in red and melanised focal changes. A. Scattered 16S rRNA-labelled structures in a red focal change, appearing within intact myocytes (arrow) and in cells in the endomysium (arrowhead). Enlarged area shows some labelled structures within the inflammatory changes. Bar = 100 µm. B. A chronic and heavily melanised change shows no labelling for 16S rRNA. Bar = 50 µm. C. Control head-kidney from fish with systemic bacterial disease, showing a severe, focal accumulation of 16S rRNA-labelled structures. Bar = 50 µm (For interpretation of the references to colour in this figure legend, the reader is referred to the web version of this article.).

melanised changes, where the information achieved by transcriptional analysis may be confusing.

MHC class I (and class II) is normally undetectable in mammalian myocytes under physiological conditions. However, MHC class I is up-regulated in certain pathological conditions, especially in inflammatory muscle diseases (Nagaraju, 2001). Studies on mammals have shown that muscle cells can act as facultative antigen-presenting cells and should be considered as active participants, rather than passive targets, of immune reactions (Nagaraju, 2001; Wiendl et al., 2005). CD8-positive T cells, *i.e.* cytotoxic T cells, and activated macrophages invade the muscle tissue and it is assumed that the auto invasive cytotoxic T cells recognise muscle-derived self-peptide antigens presented in MHC class I on the myocyte surface, causing necrosis (Wiendl et al., 2005). We hypothesized that this could be the case also with the onset of the inflammatory condition in salmon muscle, but we never detected MHC class I positive myocytes in the focal red changes where myocyte necrosis was abundant. We therefore consider it unlikely that MHC class I-driven myositis is the initial process in the pathogenesis of red focal changes.

Previous investigations using different staining procedures have

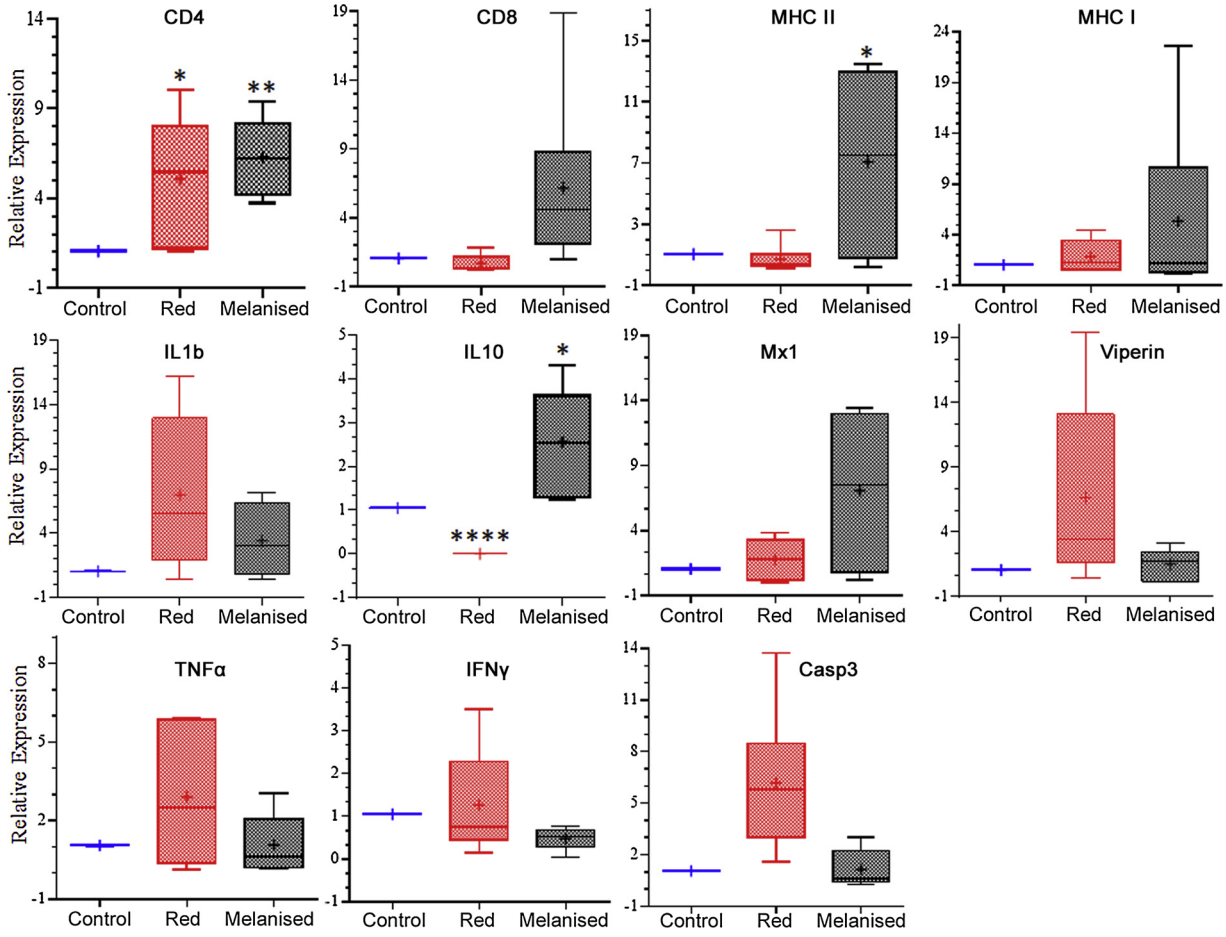

Fig. 7. RT-qPCR of selected genes in control muscle and in red and melanised focal changes. Bar graphs showing relative fold change of mRNA expression of CD4-2a, CD8, MHC class II, MHC class I, IL1b, IL10, Mx1,Viperin, TNFα, IFNγ and Casp3 in focal red (red bars) and melanised (dark grey bars) changes and control muscle (blue bars) from the same individuals normalized against EF1AB. The asterisks represent a significant difference from the control (****$p < 0.0001$, **$p < 0.01$ & *$p < 0.05$) (For interpretation of the references to colour in this figure legend, the reader is referred to the web version of this article.).

never revealed bacteria in the changes (Bjørgen et al., 2019, 2015; Koppang et al., 2005; Larsen et al., 2012). However, bacteria have been suggested by others to be a component in the pathogenesis of focal muscle changes (Krasnov et al., 2016). Therefore, the sensitive technique of ISH (RNAscope©, ACD Bio) targeting 16S rRNA, a universally conserved target for detection of bacterial RNA, was performed in parallel with Gram stained sections to detect the possible presence of bacteria. In red and melanised changes, scattered bacteria-like 16S rRNA structures were occasionally seen within seemingly un-affected myocytes and in cells in the endomysium; however, we were not able to verify these results with Gram staining. The appearance and distribution of 16S rRNA-positive signals could very well be bacteria-like structures; however, the positive signals were not seen in relation to the pathological changes. The presence of 16S rRNA-positive structures in the periphery of the tissue sections were interpreted as bacterial contamination following sampling. This, in addition to the generally low presence or total absence of detection in most samples, indicates that bacteria are not involved in the pathogenesis of focal muscle changes. Replicating virus, however, was constantly found within granulomatous, melanised changes, and was a feature consistent with the chronic nature of the condition which is in accordance with our previous findings (Bjørgen et al., 2019). The μNS PRV staining was observed mainly in macrophage-like cells, indicating that the virus is able to replicate in the scavenger cells in an inflammatory focus. The increase in Viperin and Mx expression in red and black changes, respectively, indicate a dominating anti-viral response. In addition, the expression of Caspase3, which plays an essential role in apoptosis, increased in acute red changes. This might be an attempt to prevent viral infection and replication, as apoptosis is a common host defense strategy in several viral infections (Orzalli and Kagan, 2017).

The progression from acute red to chronic melanised changes was demonstrated by the shift in the inflammatory response. The innate immune genes investigated included several pro- and anti-inflammatory interleukins (IL1β, TNFα, IFNγ and IL10) chosen based on their role in inflammatory and anti-inflammatory reactions in fish (Secombes et al., 2011). Genes encoding for adaptive immune molecules included markers for both non-professional and professional antigen-presenting cells (MHC class I and II) and genes for T cell surface proteins (CD4 and CD8). Trends in the RT-qPCR results showed that innate immune parameters were generally more highly expressed in the acute red changes, while expression of adaptive immune parameters was generally higher in the chronic melanised changes. The strong and statistically significant downregulation of IL10 in the red changes was a major finding in these investigations. Our results reveal the importance of this immune parameter as a key regulator of the immune responses in this condition. As the function of IL10 is downregulation of immune responses, its absence of expression in the acute changes indicates a swift onset of defense mechanisms as a response to the observed injury. Concurrent trends were seen in the expression of several pro-inflammatory cytokines (TNFα, IFNγ and IL1) which were generally higher expressed in red focal changes, though not statistically significant. Among previous studies reporting on IL10 in teleost fish, Collet et al. (Collet et al., 2015) investigated the expression of IL10 in Atlantic salmon peripheral blood following experimental infection with infectious salmon anemia virus (ISAV) showing induction at a late stage of the infection. Similarly, Ingerslev et al. (Ingerslev et al., 2009) found a significant upregulation of IL10 24 days post an intraperitoneal challenge with infectious pancreatic necrosis virus (IPNV). Both of these studies seem to correspond well with our results, where IL10 was downregulated in all red changes followed by an upregulation in all melanised changes. Importantly, both above-mentioned studies were controlled experiments with fish in the same phase of the infection. In our case, the samples were not obtained in a controlled experimental environment, meaning that the fish was selected only on the basis of presence of different muscle changes, and their infection history was unknown. Therefore, we cannot exclude the effects of other pathogens or external factors, despite all fish being PRV infected. However, we know from a previous study that red changes can occur without virus infection and that the impact of PRV appears to be more important in severely melanised changes (Bjørgen et al., 2019). Nevertheless, our results are highly consistent, pointing to a significant role of IL10 in the condition.

In conclusion, the red focal changes are dominated by haemorrhage and myocyte necrosis. A prominent downregulation of IL10 was seen in all red changes. PRV was present and shown to replicate in the changes. The impact of the virus is uncertain, and this study cannot conclude with respect to causes for the onset of the condition. Nevertheless, the possibility of MHC class I-driven myositis seems unlikely as IHC targeting MHC class I was negative in myocytes in all red focal changes. The immunopathological characterization of red focal changes supports the notion that the red focal changes are an acute form that develops into a chronic inflammation where granulomas with replicating PRV are a consistent feature.

Authors' contributions

HB: Planning, sampling of material, histological experiments and analysis and writing of manuscript; KS: RT-qPCR analysis and commented on the manuscript; GG: Histological analysis and commented on the manuscript. CMP: Planning and commented on the manuscript. ER: Planning and commented on the manuscript; EOK: Planning, sampling of material, commenting on the manuscript and co-ordinating the overall work.

Declaration of Competing Interest

The authors declare that they have no competing interests.

Acknowledgements

The Norwegian Seafood Research Fund (FHF) is acknowledged for funding (Grant number 901501). The project reference group consisting of Kristian Prytz (FHF), Øyvind Oaland (Mowi ASA), Geir Magne Knutsen (Seaborn ASA), Erlend Haugarvoll (Lingalaks) and Line Rønning (Lerøy ASA) are acknowledged for fruitful discussions throughout the project period. Ms. Clementine Linde is acknowledged for laboratory assistance. Dr. Øystein Wessel is acknowledged for valuable comments on the manuscript.

References

Aas, I.B., Austbø, L., König, M., Syed, M., Falk, K., Hordvik, I., Koppang, E.O., 2014. Transcriptional characterization of the T cell population within the salmonid interbranchial lymphoid tissue. J. Immunol. 193, 3463–3469.

Aas, I.B., Austbø, L., Falk, K., Hordvik, I., Koppang, E.O., 2017. The interbranchial lymphoid tissue likely contributes to immune tolerance and defense in the gills of Atlantic salmon. Dev. Comp. Immunol. 76, 247–254.

Austbø, L., Aas, I.B., König, M., Weli, S.C., Syed, M., Falk, K., Koppang, E.O., 2014. Transcriptional response of immune genes in gills and the interbranchial lymphoid tissue of Atlantic salmon challenged with infectious salmon anaemia virus. Dev. Comp. Immunol. 45, 107–114.

Bjørgen, H., Wessel, O., Fjelldal, P.G., Hansen, T., Sveier, H., Saebø, H.R., Enger, K.B., Monsen, E., Kvellestad, A., Rimstad, E., Koppang, E.O., 2015. *Piscine orthoreovirus* (PRV) in red and melanised foci in white muscle of Atlantic salmon (*Salmo salar*). Vet. Res. 46, 89.

Bjørgen, H., Haldorsen, R., Oaland, Ø., Kvellestad, A., Kannimuthu, D., Rimstad, E., Koppang, E.O., 2019. Melanized focal changes in skeletal muscle in farmed Atlantic salmon after natural infection with *Piscine orthoreovirus* (PRV). J. Fish Dis. 42, 935–945.

Boardman, T., Warner, C., Ramirez-Gomez, F., Matrisciano, J., Bromage, E., 2012. Characterization of an anti-rainbow trout (*Oncorhynchus mykiss*) CD3ε monoclonal antibody. Vet. Immunol. Immunopathol. 145, 511–515.

Collet, B., Urquhart, K., Monte, M., Collins, C., Perez, S.G., Secombes, C.J., Hall, M., 2015. Individual monitoring of immune response in Atlantic Salmon *Salmo salar* following experimental infection with infectious salmon anaemia virus (ISAV). PLoS One 10, e0137767.

Dalakas, M.C., 2015. Inflammatory muscle diseases. N. Engl. J. Med. 372, 1734–1747.

Finstad, Ø.W., Falk, K., Løvoll, M., Evensen, Ø., Rimstad, E., 2012. Immunohistochemical detection of *piscine reovirus* (PRV) in hearts of Atlantic salmon coincide with the course of heart and skeletal muscle inflammation (HSMI). Vet. Res. 43, 27.

Finstad, Ø.W., Dahle, M.K., Lindholm, T.H., Nyman, I.B., Løvoll, M., Wallace, C., Olsen, C.M., Storset, A.K., Rimstad, E., 2014. *Piscine orthoreovirus* (PRV) infects Atlantic salmon erythrocytes. Vet. Res. 45, 35.

Haatveit, H.M., Nyman, I.B., Markussen, T., Wessel, Ø., Dahle, M.K., Rimstad, E., 2016. The non-structural protein μNS of *piscine orthoreovirus* (PRV) forms viral factory-like structures. Vet. Res. 47, 5.

Hetland, D.L., Jørgensen, S.M., Skjødt, K., Dale, O.B., Falk, K., Xu, C., Mikalsen, A.B., Grimholt, U., Gjøen, T., Press, C.M., 2010. In situ localisation of major histocompatibility complex class I and class II and CD8 positive cells in infectious salmon anaemia virus (ISAV)-infected Atlantic salmon. Fish Shellfish Immunol. 28, 30–39.

Hetland, D.L., Dale, O.B., Skjødt, K., Press, C.M., Falk, K., 2011. Depletion of CD8 alpha cells from tissues of Atlantic salmon during the early stages of infection with high or low virulent strains of infectious salmon anaemia virus (ISAV). Dev. Comp. Immunol. 35, 817–826.

Ingerslev, H.C., Rønneseth, A., Pettersen, E., Wergeland, H., 2009. Differential expression of immune genes in Atlantic salmon (*Salmo salar* L.) challenged intraperitoneally or by cohabitation with IPNV. Scand. J. Immunol. 69, 90–98.

Koppang, E.O., Haugarvoll, E., Hordvik, I., Aune, L., Poppe, T.T., 2005. Vaccine-associated granulomatous inflammation and melanin accumulation in Atlantic salmon, *Salmo salar* L., white muscle. J. Fish Dis. 28, 13–22.

Krasnov, A., Moghadam, H., Larsson, T., Afanasyev, S., Mørkøre, T., 2016. Gene expression profiling in melanised sites of Atlantic salmon fillets. Fish Shellfish Immunol. 55, 56–63.

Larsen, H.A., Austbø, L., Mørkøre, T., Thorsen, J., Hordvik, I., Fischer, U., Jirillo, E., Rimstad, E., Koppang, E.O., 2012. Pigment-producing granulomatous myopathy in Atlantic salmon: a novel inflammatory response. Fish Shellfish Immunol. 33, 277–285.

Løvoll, M., Alarcón, M., Jensen, B.B., Taksdal, T., Kristoffersen, A.B., Tengs, T., 2012. Quantification of *piscine reovirus* (PRV) at different stages of Atlantic salmon Salmo salar production. Dis. Aquat. Org. 99, 7–12.

Mørkøre, T., Larsson, T., Kvellestad, A.S., Koppang, E.O., Åsli, M., Krasnov, A., Dessen, J.E., Moreno, H.M., Valen, E.C., Gannestad, K.H., 2015. Mørke flekker i laksefilet. Kunnskapsstatus og tiltak for å begrense omfanget (Melanised changes in salmon fillet. Knowledge status and efforts to limit their occurrence). Nofima report series 34 (2015).

Moldal, T., Løkka, G., Wiik-Nielsen, J., Austbø, L., Torstensen, B.E., Rosenlund, G., Dale, O.B., Kaldhusdal, M., Koppang, E.O., 2014. Substitution of dietary fish oil with plant oils is associated with shortened mid intestinal folds in Atlantic salmon (*Salmo salar*). BMC Vet. Res. 10, 60.

Nagaraju, K., 2001. Immunological capabilities of skeletal muscle cells. Acta Physiol. Scand. 171, 215–223.

Olsvik, P.A., Lie, K.K., Jordal, A.-E.O., Nilsen, T.O., Hordvik, I., 2005. Evaluation of potential reference genes in real-time RT-PCR studies of Atlantic salmon. BMC Mol. Biol. 6, 21.

Orzalli, M.H., Kagan, J.C., 2017. Apoptosis and necroptosis as host defense strategies to prevent viral infection. Trends Cell Biol. 27, 800–809.

Secombes, C.J., Wang, T., Bird, S.J.D., 2011. The interleukins of fish. C. Immunology 35 (12), 1336–1345.

Wang, F., Flanagan, J., Su, N., Wang, L.-C., Bui, S., Nielson, A., Wu, X., Vo, H.-T., Ma, X.-J., Luo, Y., 2012. RNAscope: a novel *in situ* RNA analysis platform for formalin-fixed, paraffin-embedded tissues. J. Mol. Diagn. 14, 22–29.

Wessel, Ø., Braaen, S., Alarcon, M., Haatveit, H., Roos, N., Markussen, T., Tengs, T., Dahle, M.K., Rimstad, E., 2017. Infection with purified Piscine orthoreovirus demonstrates a causal relationship with heart and skeletal muscle inflammation in Atlantic salmon. PLoS One 12 (8), e0183781.

Wiendl, H., Hohlfeld, R., Kieseier, B.C., 2005. Immunobiology of muscle: advances in understanding an immunological microenvironment. Trends Immunol. 26, 373–380.